JOURNAL OF MATERIALS SCIENCE 21 (1986) 1879–1888

Work of fracture of unidirectional metal matrix composites subjected to isothermal exposure

TETSUYUKI KYONO*, IAN W. HALL, MINORU TAYA‡
Department of Mechanical and Aerospace Engineering, University of Delaware, Newark, Delaware 19716, USA

Work of fracture, γ_F, was measured on as-fabricated and isothermally exposed unidirectional boron fibre reinforced 1100 aluminium composites. Then an analytical study was made to predict γ_F of unidirectional metal matrix composites with the special emphasis on the thermally degraded composites. In the analytical study the statistical data on the strength of the fibres that were extracted from as-fabricated and thermally exposed composites were used. A good agreement between the experimental and analytical results of γ_F was obtained for the entire range of exposure time. It was found in this study that the toughness of the thermally exposed composite decreases with the increase in the exposure time.

1. Introduction

Metal matrix composites (MMCs) are superior to polymer matrix composites in demanding environments, particularly at elevated temperature. Thus, the maintenance of undegraded mechanical properties in an MMC that undergoes temperature excursions is vitally important if the MMC is to be used as a high temperature material. Temperature excursions include not only the thermal loading which the MMC is designed to suffer in use, but also the past thermal history that MMC has undergone durings its fabrication. It is known that temperature excursions affect the matrix–fibre interfacial strength and, thus, the strength of the composite [1–7]. DiCarlo [7] developed a theoretical model to predict the strength of MMCs subjected to isothermal exposure. In DiCarlo's model, the formation of intermetallic compounds at the fibre–matrix interface played a very important role.

Though the stiffness and strength of MMCs have always been focused on as primary properties, the toughness of MMCs must be considered to be equally important for some applications. Unfortunately, these three properties often conflict with each other. It has been reported [8–14] that the concept of stress intensity factor, K_{IC}, based on linear fracture mechanics, is not applicable to most composites, particularly continuous fibre composites, and microscopic fracture modes which are characteristic of fibres, for example fibre pull-out, should be considered in estimation of toughness. A number of researchers have used a three-point bending test to measure the toughness of MMCs [15–19]. This method was first explored by Nakayama [20] who used a centre notched specimen and was later modified by Tattersall and Tappin [21] who used a triangular ligament at the mid-point. The toughness measured by a three-point bending test is called "work of fracture" (γ_F). Taya and his co-workers have recently proposed an analytical model to predict γ_F [18, 22] and achieved good agreement between the analytical and experimental results for continuous fibre MMCs [18] and short fibre MMCs [19]. In Taya and Daimaru's [18] work, however, the effect of temperature excursions on the work of fracture was not considered.

In this paper, we will focus on the effect of isothermal exposure on the room temperature value of γ_F of a continuous fibre MMC. To this end both analytical and experimental work have been conducted. The analytical model to account for the effect of thermal exposure will be stated in Section 2 followed by the experimental procedure in Section 3. Then, the experimental results and their comparison with the analytical ones will be described in Section 4. Finally, the conclusions which may be drawn are enumerated in Section 5.

2. Analytical model

The analytical model developed by Taya and his coworkers [18, 19, 22] is modified here to account for the effect of thermal exposure. Thus, only the formulation relevant to the effect of thermal exposure will be stated in detail here. Otherwise, the description of the model of Taya *et al.* is only presented in outline, except for modification.

It was found [18] that three mechanisms can contribute to the total fracture energy, W_F, of a three-point bending test specimen with a triangular ligament; elastic strain energy, plastic work along the fibre–matrix interface and fibre pull-out energy. In the formulae describing these three contributions, the fibre ultimate tensile strength, σ_{fu}, (hereafter referred to as fibre strength) plays an important role and σ_{fu} is strongly dependent on the thermal exposure temperature (T) and exposure time (t). Thus, we will first

*On leave from Toray Industries, Inc., Otsu, Shiga 520, Japan.
‡*Present address*: Department of Mechanical Engineering, University of Washington, Seattle, WA 98195, USA.

0022–2461/86 $03.00 + .12

describe the effect of T and t on σ_{fu}, then the three contributions to W_F followed by the formula for γ_F.

2.1. Effect of thermal exposure time (t) and temperature (T) on the fibre strength (σ_{fu})

It is well known that reaction products frequently form at the interface when an MMC is exposed to elevated temperature, resulting in the loss of fibre strength, which in turn causes a reduction in the composite strength and toughness. DiCarlo [7] conducted a model study on an aluminium coated boron fibre and found that a Griffith-type fracture model could predict well the reduction in the average fibre strength of an aluminium coated boron fibre. The thickness of the reaction product can be given by [7]

$$h = \alpha t^{1/2} \exp\left[-Q/2kT\right] \tag{1}$$

where α is a normalizing constant, t is exposure time, T is exposure temperature in Kelvin, k is Boltzmann's constant, and Q is the activation energy controlling product growth.

Based on the Griffith theory, Metcalfe and Klein [1] obtained the fibre strength σ_{fu} as

$$\sigma_{fu} = \begin{cases} \sigma^n_{fu} & \text{for } \sigma^n_{fu} \leqslant \sigma^r_f \\ \sigma^r_{fu} = B/h^{\frac{1}{2}} & \text{for } \sigma^n_{fu} > \sigma^r_f \end{cases} \tag{2}$$

where σ^n_{fu} and σ^r_{fu} are the tensile strength of a non-reacted and reacted fibre, respectively, and B is a material constant. By substituting Equation 1 into Equation 2, the tensile strength of a reacted fibre, σ^r_{fu}, which is set equal to σ_{fu} in our study, is now given by

$$\sigma_{fu} = ct^{-\frac{1}{4}} \exp\left(\frac{Q}{4kT}\right) \tag{3}$$

where c is an empirically determined constant. For the case of a boron/aluminium composite, σ^r_{fu} (in GPa) can be expressed as

$$\sigma_{fu} = 3.5 \times 10^{-4} t^{-\frac{1}{4}} \exp\left(\frac{7060}{T}\right) \tag{4}$$

where the following values were used [1, 7]:

$$\begin{aligned} Q &= 3.90 \times 10^{-19}\,\text{J} \\ k &= 1.38 \times 10^{-23}\,\text{J K}^{-1} \\ B &= 1.59 \times 10^{6}\,\text{N m}^{-\frac{3}{2}} \\ c &= 3.5 \times 10^{5}\,\text{N m}^{-2}\,\text{h}^{\frac{1}{4}} \\ \alpha &= 20.7\,\text{m h}^{-\frac{1}{2}} \end{aligned} \tag{5}$$

2.2. Work of fracture, γ_F

Work of fracture, γ_F, is defined as the total fracture energy W_F during a three-point bending test divided by twice the area of the fractured section. Thus, γ_F is considered as the fracture surface energy averaged over the whole fracture process. The analytical model used in this study is basically the same as used by Taya *et al.* [18, 19] for continuous fibre MMCs, hence the detailed derivation leading to the final results will not be given here. The three energies contributing to W_F are strain energy release rate (G), plastic work (W_p) and fibre pull-out energy (W_{p0}).

The strain energy release rate, G, is given by [18]

$$G = \frac{\pi(1 - \bar{\nu}^2)\bar{\sigma}^2 a}{\bar{E}} \tag{6}$$

where a is the radius of a penny-shaped crack which is located inside a continous fibre MMC and its crack plane is perpendicular to the fibre axis; $\bar{E}$, $\bar{\sigma}$ and $\bar{\nu}$ are defined as

$$\begin{aligned} \bar{E} &= V_m E_m + V_f E_f \\ \bar{\sigma} &= V_m \sigma_m + V_f \sigma_f \\ \bar{\nu} &= V_m \nu_m + V_f \nu_f \end{aligned} \tag{7}$$

In Equation 7, V_i, E_i, σ_i and ν_i are the volume fraction, Young's modulus, average stress and Poisson's ratio of the ith phase material with i = f and m which denote fibre and matrix, respectively. Equation 6 was derived under the assumption of isostrain.

The nalytical model used in this paper to predict plastic work, W_p, is slightly different from our previous model, specifically the assumption is made in the present paper that fibres have always some weak points with an average spacing of l_w which was set equal to a critical length [10]. Then the plastic work along the matrix–fibre interface per fibre is expressed as

$$W_p = \frac{\pi d^2}{2} \delta_0 \left[(1 - \eta) \left(\frac{\sigma_{fu} + \sigma^*}{2} - \sigma_{f0} \right) + \eta(\sigma_{fu} - \sigma_{f0}) \right] \tag{8}$$

where d is the fibre diameter; σ_{fu}, σ^* and σ_{f0} are respectively, the fibre strength (σ_{fu}) defined by Equation 2, the fibre strength at weak points and the average fibre stress when the composite fractures; δ_0 is the crack opening displacement (COD) at the fibre location [23] and its detailed expression is given by Taya and Daimaru [18], and η is defined by

$$\eta = \frac{\sigma^*}{\sigma_{fu}} \tag{9}$$

It is assumed in this study that σ^* is set equal to the fibre bundle strength, σ_B, which is related to the Weibull modulus ω as [24]

$$\sigma_B = \sigma_{fu} \left[\omega^{\frac{1}{\omega}} \exp\left(\frac{1}{\omega}\right) \Gamma\left(1 + \frac{1}{\omega}\right) \right]^{-1} \tag{10}$$

where Γ is Gamma function and ω can be approximated by

$$\omega = \frac{1.2}{CV} \tag{11}$$

and where CV is the coefficient of variation of the distribution of fibre strength which will be obtained by tensile tests on a number of fibre monofilaments (see Section 3.4.2.).

The formula to predict fibre pull-out energy is basically the same as that proposed by Cooper [10] and the average pull-out energy per unit fibre, W_{po}, is given by

$$W_{p0} = (1 - \eta)^3 \frac{\pi d^3 \sigma^2_{fu}}{96\tau_y} \tag{12}$$

where τ_y is the shear yield stress of the matrix and η is defined by Equation 9 and σ_{fu} by Equation 2.

The total fracture energy W_F is the sum of the strain energy release rate (G), plastic work (W_p) and fibre pull-out energy (W_{p0}), all integrated over the entire area of the fractured section (A). Work of fracture (γ_F) is defined by $W_f/2A$, and hence given by

$$\gamma_F = \frac{1}{2\pi a_f^2}\int_{a_0}^{a_f}\left\{2\pi G + \frac{8V_f}{d^2}(W_p + W_{p0})\right\} a\,da \quad (13)$$

where a_0 and a_f are the radius of a penny-shaped crack at initial and final configuration, respectively, and a_0 is given by

$$a_0 = \tfrac{1}{2}(b_0 - d) \quad (14)$$

and where b_0 is the average spacing between the centres of fibes for a hexagonal array of fibres, and a_f is the equivalent radius of fractured section defined later by Equation 20. By substituting Equations 6, 8 and 12 into Equation 13 and performing the integration with respect to a, then neglecting the higher order terms, we arrive at

$$\gamma_F = \frac{1}{2}\left[\frac{2\pi(1-\bar{\nu}^2)\bar{\sigma}a_f}{3\bar{E}}(1+\alpha+\beta) + (1-\eta)^3\frac{dV_f\sigma_{fu}^2}{24\tau_y}\right] \quad (15)$$

where

$$\alpha = \frac{2(1-\eta)(\sigma_{fu}+\sigma^*-2\sigma_{f0})(\sigma_{fu}+\sigma^*)\bar{E}}{\pi\bar{\sigma}^2E_m} \times\left[\frac{4}{5}\left(\frac{\bar{\sigma}}{\sigma_{fu}+\sigma^*}\right)\left(\frac{a_0}{a_f}\right)^{1/2} - \frac{1}{2\pi}\left(\frac{d}{a_f}\right)\right] \quad (16)$$

$$\beta = \frac{8\eta(\sigma_{fu}-\sigma_{f0})\sigma_{fu}\bar{E}}{\pi\bar{\sigma}^2E_m}\left[\frac{2}{5}\left(\frac{\bar{\sigma}}{\sigma_{fu}}\right)\left(\frac{a_0}{a_f}\right)^{1/2} - \frac{1}{2\pi}\left(\frac{d}{a_f}\right)\right] \quad (17)$$

3. Experimental procedure

Several thermal treatments, mechanical tests and metallographic study were made on boron fibres and boron fibre/1100 aluminium (B/Al for short) composites. We will describe the experimental procedure for each test or study below.

3.1. Material

B/Al composites, supplied by AVCO Speciality Material Division, Lowell, MA, were chosen for study and two different volume fractions of fibres were chosen; $V_f = 0.3$ and 0.5. The mechanical properties of boron fibre and 1100 aluminium are given as

$$\begin{aligned}\text{boron fibre:}\quad d &= 1.02\times10^{-4}\,\text{m}\\ \sigma_{fu} &= 3520\,\text{MPa}\\ E_f &= 400\,\text{GPa}\\ \nu_f &= 0.18\ [25]\end{aligned} \quad (18)$$

$$\begin{aligned}\text{1100 aluminium:}\quad \sigma_{mu} &= 90\,\text{MPa}\\ E_m &= 69\,\text{MPa}\\ \tau_y &= 20\,\text{MPa}\\ \nu_m &= 0.33\end{aligned} \quad (19)$$

The reason why 1100 aluminium was chosen as a matrix metal was to avoid the presence of any second phase or precipitate particles in the matrix. The B/Al composite plates were fabricated by a diffusion bonding method and two different plies were used, 8 plies for tensile tests and 42 plies for three-point bending tests.

3.2. Isothermal exposure test

B/Al composites samples were exposed to 500° C in argon for times (t) of 1, 8, 24 or 72 h. Although 500° C is considerably higher than any conceivable temperature which might be met in service, this temperature was chosen as it is known to be sufficient to cause marked changes in the tensile properties of the composite [6] and should allow rapid formation of fibre/matrix interfacial reaction products.

3.3. Metallography

Samples of as-fabricated and thermally exposed material were examined by optical microscopy for evidence of any effect of the thermal exposure treatment. No effect was discernible, consequently, samples were sectioned perpendicular to the fibre axis and prepared for examination in a Philips EM 400T transmission electron microscope (TEM); 3 mm diameter discs were trepanned from the composite, mechanically ground to $< 70\,\mu$m and ion-milled at 4 keV until perforation.

3.4. Tensile tests

3.4.1. Composites

Longitudinal tensile tests were carried out on both as-fabricated and isothermally exposed composites. Specimens were 152.4 mm long, 12.7 mm wide and 1.24 mm thick for $V_f = 0.3$, and 0.88 mm thick for $V_f = 0.5$, respectively. Strain gauges were applied to the mid-length of the specimen gauge length, which was 76.2 mm, and aluminium end-tabs were adhesively bonded to each side of the specimen in the grip area. All tests were conducted at room temperature by using a standard Instron machine at a strain rate of $6.7\times10^{-3}\,\text{min}^{-1}$. This test provided us with complete data on the stress–strain curve of the composite.

3.4.2. Fibres

In order to obtain the ultimate tensile strength, σ_{fu}, and Weibull modulus, ω, of thermally exposed fibres, boron fibres were extracted from a thermally exposed composite by using 10% NaOH [26]. Then tensile tests were conducted on 50 fibres for each thermal condition by using a standard Instron machine with pneumatic action grips. The fibres were held between papers to prevent breakage in the grips. A strain rate of $5\times10^{-3}\,\text{min}^{-1}$ was employed. These tests provided us with the distribution of fibre strength, from which the Weibull modulus was computed.

3.5. Three-point bending test

Three-point bending tests were conducted on both as-fabricated and thermally exposed composites in order to measure γ_F. The configuration of the three-point bending test is shown in Fig. 1. The specimen

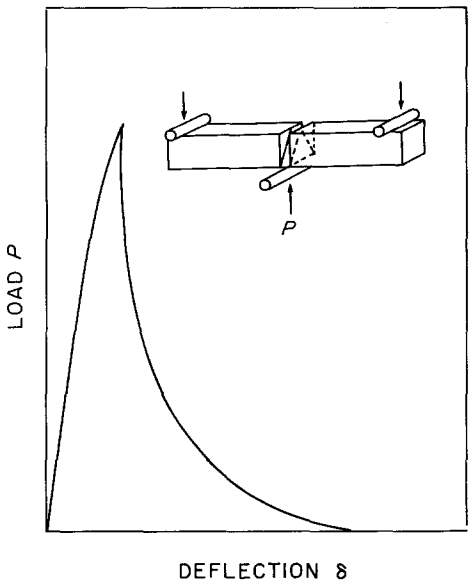

Figure 1 Three-point bending test and load (P) against displacement (δ) curve used to obtain the fracture energy (W_F).

size was 76.2 mm long, 6.10 mm wide and 6.10 mm thick for $V_f = 0.3$, and 4.06 mm thick for $V_f = 0.5$. The ligament in the centre is an isosceles triangle, and slits were cut by using an 0.864 mm thick diamond wheel. The slit plane is parallel to the plane of the triangular sections. Specimens were mounted in a three-point bending fixture with a span length of 63.5 mm, then were loaded to failure by using a standard Instron testing machine at a crosshead speed of 1.27 mm min^{-1}. Upon loading, a crack was initiated from the apex of the triangular section and propagated in a well-controlled manner until complete fracture of the specimens. At the same time, load (P) against deflection (δ) curves, illustrated schematically in Fig. 1, were recorded. Then, the area under the curve, which is considered to be equal to the total energy absorbed during the whole fracture process, W_F, was measured. Then work of fracture γ_F was computed by $\gamma_F = W_F/2A$, where A is the area of the triangular section. Three tests were conducted on thermally exposed composite for each exposure time.

4. Experimental results and discussion

4.1. Metallography

Although optical microscopy yielded little information, the TEM observations are believed to be of critical importance in this work. It became clear during specimen preparation that the diffusion bonding process had not been successful in producing a monolithic matrix because delamination was visible between the 1 1 0 0 Al sheets and, in particular, at the "triple point" shown in the fibre/matrix interface in Fig. 2. Examination of the interface between sheets showed that a thin microcrystalline layer was present and that this layer effectively delineated the original diffusion bonded joint, Fig. 3. Electron diffraction patterns from this layer yield weak spotty rings, the majority of which can be indexed as arising from Al_2O_3.

At the fibre/matrix interface itself, contact was generally poor and limited to a few regions around the periphery of the fibre. Clearly it is not known to what extent the sample preparation procedure affects the appearance of the fibre/matrix interface but, firstly, the observations are consistent with those made by optical microscopy and, secondly, no evidence of radiation-induced defects was noted.

At those regions where the fibre and matrix were in intimate contant the same interfacial alumina layer, as noted betwen 1 1 0 0 Al sheets, was present and Fig. 4 shows the general features of these regions in a sample which had been thermally exposed for 72 h at 500° C. Micro-microdiffraction patterns from regions on either

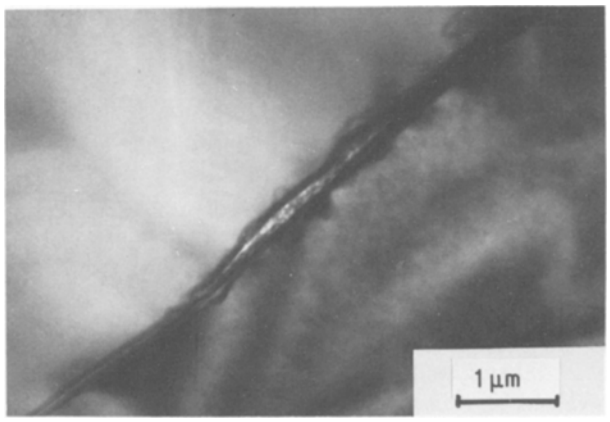

Figure 3 Transmission electron micrograph of the interface between 1 1 0 0 Al sheets showing thin oxide layer trapped between sheets.

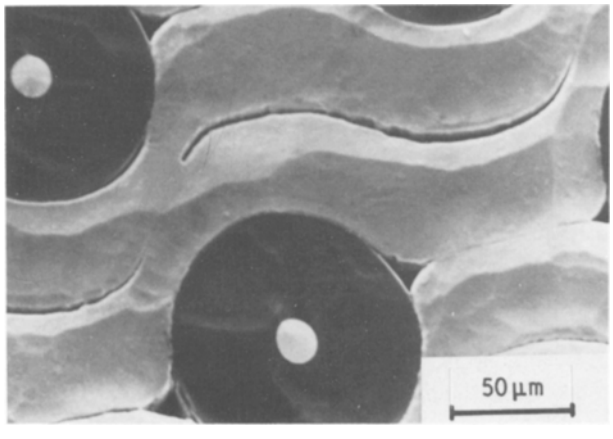

Figure 2 Scanning electron micrograph of an ion-milled sample showing clearly the interfaces between 1 1 0 0 Al sheets.

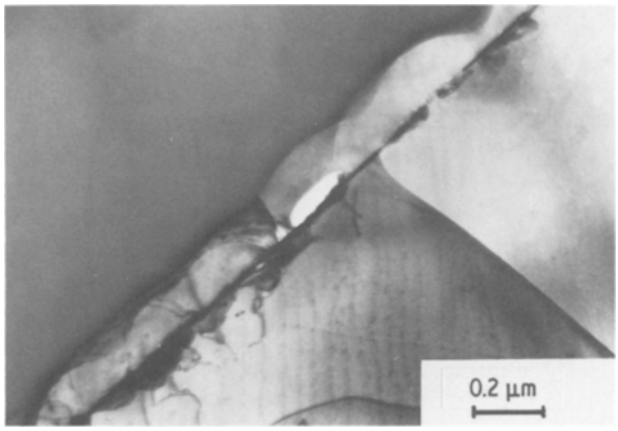

Figure 4 Transmission electron micrograph showing fibres/matrix interface in sample thermally exposed for 72 h. Note the thin trapped oxide layer similar to that in Fig. 3.

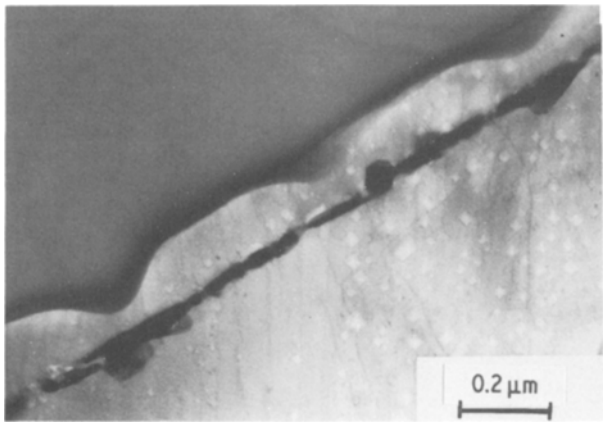

Figure 5 Transmission electron micrograph of sample thermally exposed for 72 h, showing cusps associated with the larger crystals at the original fibre/matrix interface.

side of the alumina layer (e.g. regions marked X on Fig. 4) show that both are single crystal aluminium with a slight relative misorientation of $\sim 5°$. Several larger crystals are observed at the alumina interfacial layer and convergent beam diffraction patterns indicate that these are probably AlB_2.

Since it is commonly assumed and has been reported that an interfacial reaction occurs between the boron fibres and aluminium matrix, the above observations are somewhat surprising since nothing resembling an interfacial layer of reaction product is visible in TEM. If the alumina layer does indeed mark the original fibre/matrix interface, then Fig. 4 shows that there has been a net diffusion of aluminium into the boron fibre. It is noted that the advancing Al/B boundary is not planar but contains many cusps and that these cusps correspond to the larger crystals in the alumina layer. This is shown very clearly in Fig. 5.

On the basis of the above observations it is concluded that the alumina layer acts as a diffusion barrier between the aluminium matrix and boron fibre since the cusps indicate that penetration is more rapid where the alumina layer is thinnest. The alumina layer presumably also prevents good fibre/matrix or matrix/

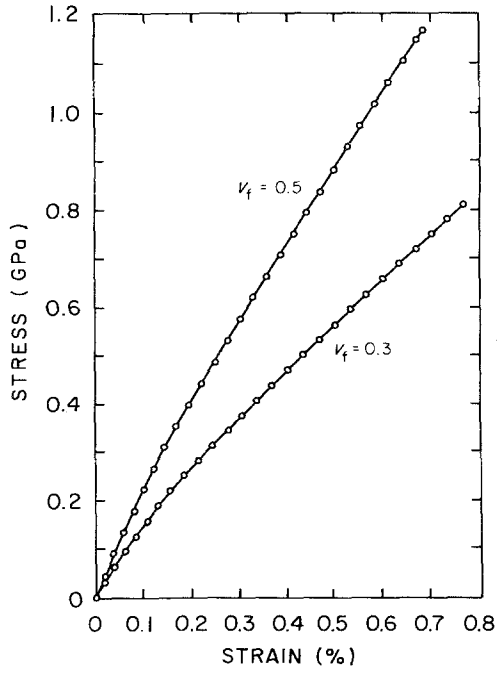

Figure 6 Stress-strain curves of as-received B/Al composites for $V_f = 0.3$ and 0.5.

matrix contact or wetting. The absence of the anticipated extensive reaction zone between fibre and matrix is, therefore, believed to be a consequence of the presence of the diffusion barrier.

4.2. Tensile tests

4.2.1. Composite

Typical stress–strain curves of as-fabricated composites are shown in Fig. 6 for $V_f = 0.3$ and 0.5, and the variation of ultimate tensile strength (σ_c) of the composite with exposure time (t) is shown graphically in Fig. 7. The values of Young's modulus, E_c, turned out to be independent of exposure time for $V_f = 0.3$ and 0.5 and are about 90% and 92% of those calculated by the rule of mixture, respectively. It is noted from Fig. 7 that σ_c for $V_f = 0.3$ and 0.5 are about 56% and 69% of the rule of mixture value of as-fabricated composite, and σ_c decreases with the increase of t and

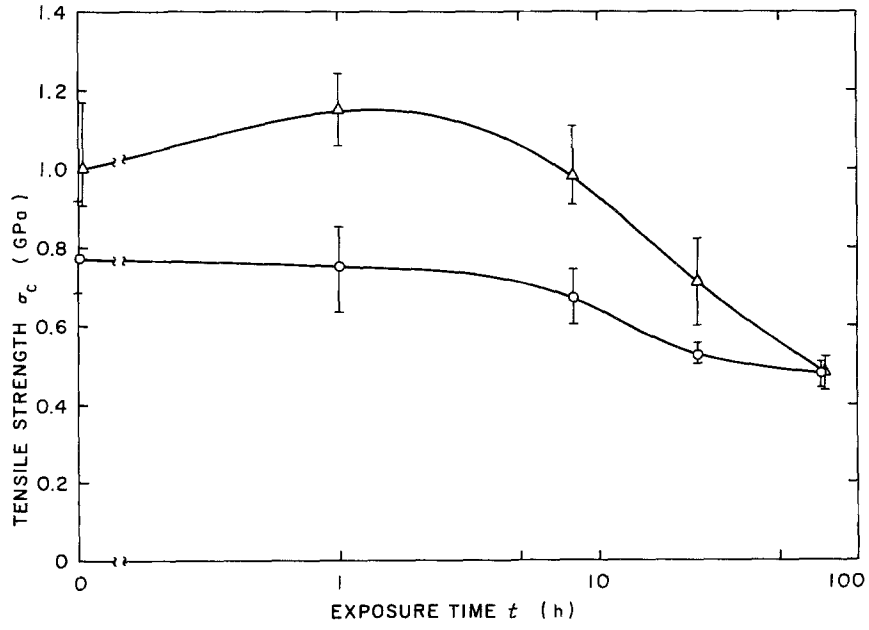

Figure 7 Tensile strength (σ_c) of thermally exposed B/Al as a function of exposure time (t) at 500° C. (○) $V_f = 30$, (△) $V_f = 50$.

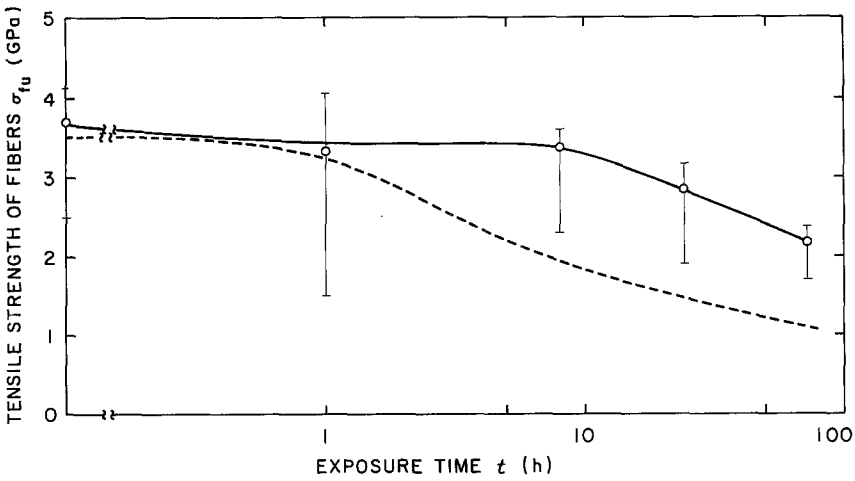

Figure 8 Tensile strength (σ_{fu}) of boron fibres extracted from as-received and thermally exposed composite. (○) Experimental values, (– – –) prediction by DiCarlo's model.

approaches a constant value at and beyond 72 h, which is 62% (48%) for $V_f = 0.3$ (0.5), of the as-fabricated composite. It is also noted from Fig. 7 that σ_c for $V_f = 0.5$ increases slightly at $t = 1$ hour, which will be discussed in the following section.

4.2.2. Fibres

The results of the tensile tests on as-received and as thermally-exposed fibres are shown as a solid curve with experimental error band in Fig. 8. As-exposed fibres were extracted from composites that were subjected to isothermal exposure at $T = 500°$ C. The results of fibre strength predicted by Equation 4 are also plotted as a dashed curve in Fig. 8. It is obvious from Fig. 8 that the fibre strength decreases with increasing exposure time (t) due to the formation of the reaction product which was identified as AlB_2 by X-ray diffraction technique [1, 27]. However, the reduction in the fibre strength measured as t increases is less than the theoretically predicted value. The discrepancy between the experimental and theoretical results is considered to be partly due to the difference of the interface condition between the present experiment and DiCarlo's idealized experiment [7]. This will be described in detail below. Empirical constants c

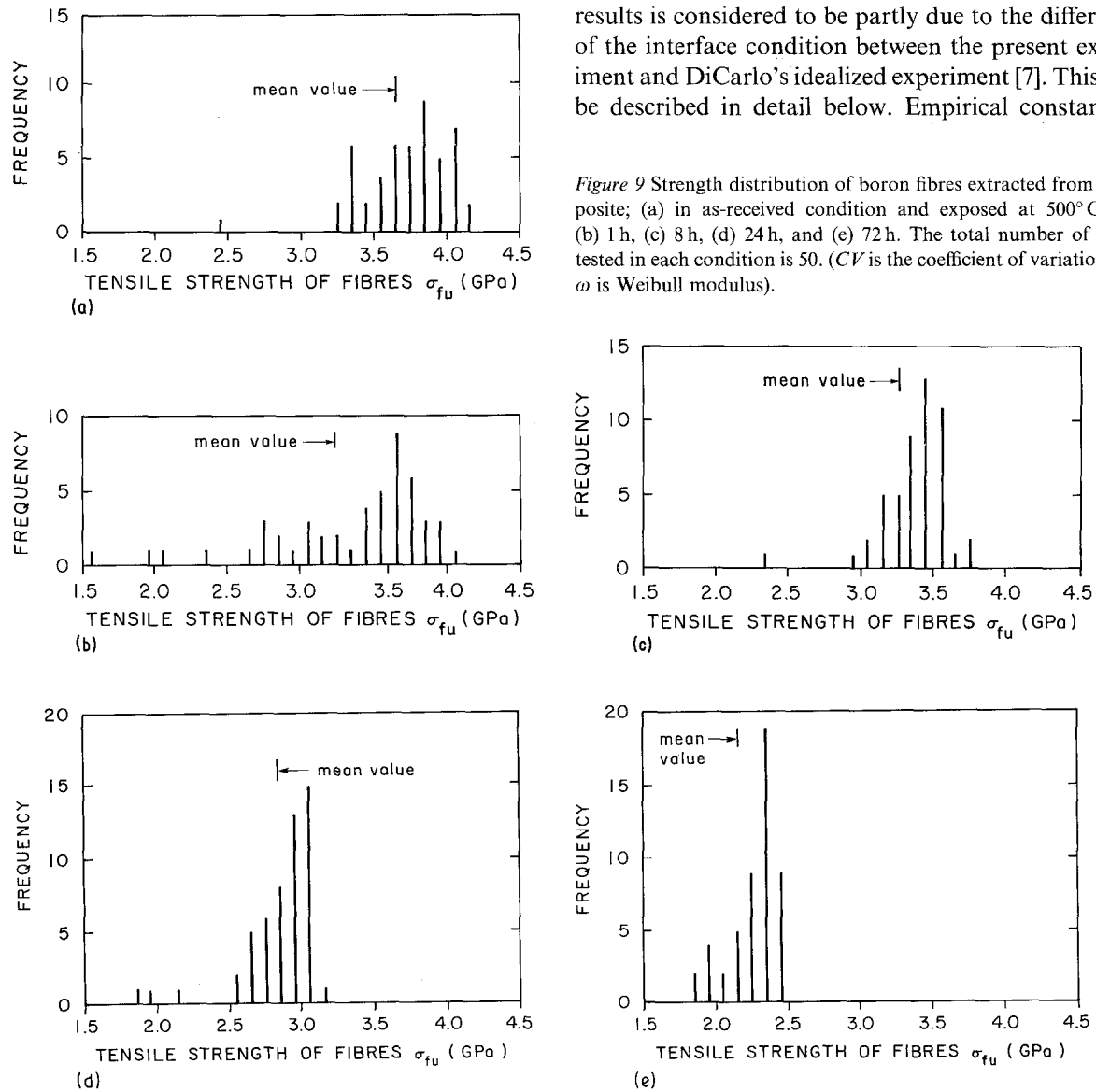

Figure 9 Strength distribution of boron fibres extracted from composite; (a) in as-received condition and exposed at 500° C for, (b) 1 h, (c) 8 h, (d) 24 h, and (e) 72 h. The total number of fibres tested in each condition is 50. (CV is the coefficient of variation and ω is Weibull modulus).

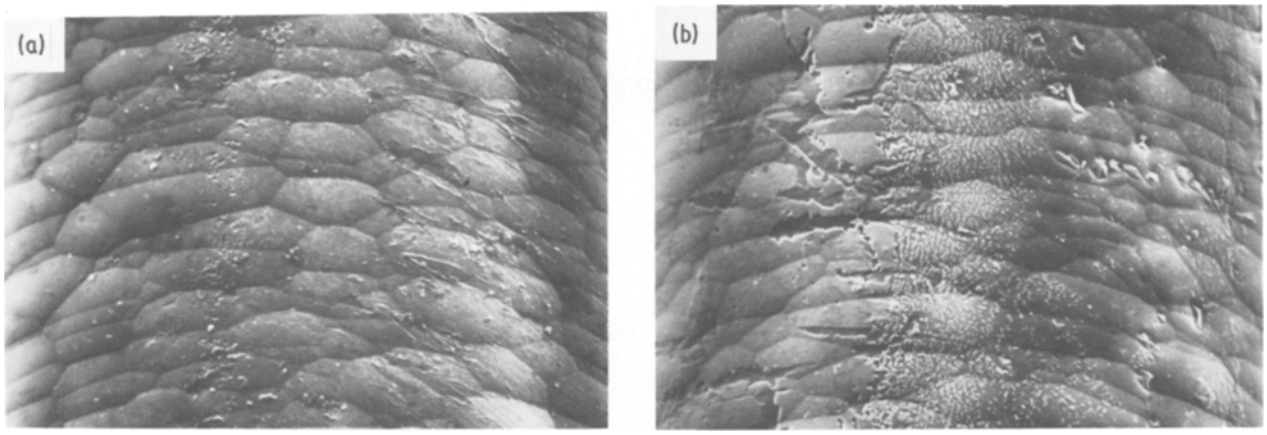

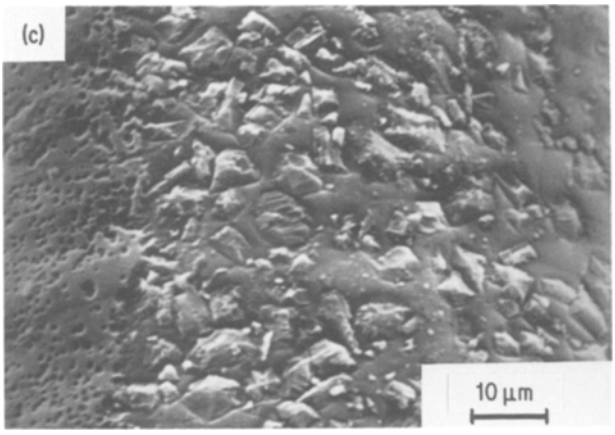

Figure 10 SEM photographs of the surfaces of boron fibres extracted from the composite, (a) as-received; (b) exposed at 500° C for 24 h; (c) 72 h.

and Q in Equation 3 are from the data in DiCarlo's experiment where a pure aluminium-coated boron fibre 203 μm in diameter was exposed at temperatures from 470° to 525° C for 1 h [7, 28]. In his experiment, the interface between boron fibre and aluminium is considered to have contained very little alumina since the pure aluminium coating was applied in vacuum at low temperature by ion-plating techniques. Therefore, the interface can be identified as a Class III system rather than the Pseudo-Class I system defined by Metcalfe and Klein [1]. On the other hand, the composite used in this study was made by diffusion bonding thin aluminium foils and boron fibres, resulting in a thin aluminium oxide layer which still remains at the interface of the isothermally exposed composite as shown in Fig. 4. It is believed that the aluminium oxide layer behaved as a diffusion barrier between the boron fibres and aluminium matrix and this makes the prediction based on DiCarlo's model inapplicable to our experimental results [29].

The strength distribution of the boron fibres is shown in Fig. 9 for t = 0 (a), 1 (b), 8 (c), 24 (d) and 72 h (e). The coefficients of variation in the fibre strength (CV) are close to those of as-received boron fibres used by DiCarlo and Smith [28], i.e. $CV = 6 \sim 10\%$ except for the value at 1 h exposure. The SEM photographs of the surfaces of fibres extracted from as-fabricated and as-thermally exposed composites are shown in Fig. 10. No significant differences were observed in surface appearance of fibres from as-fabricated composite or from the composite exposed for times up to 8 h. After 24 h exposure, occasional crystals were visible on the surface and after 72 h the surface was essentially covered with small angular crystals. These crystals are believed to be similar to those visible at the interface in Fig. 4.

4.3. Work of fracture (γ_F) by three-point bending tests

The experimentally determined values of γ_F are plotted as open circles in Fig. 11. Fig. 11 indicates that the scatter of data is large, particularly at shorter exposure times and the means values of γ_F decrease with increasing exposure time, t, except for the data of 1 h exposure. It is noted in Fig. 11 that the volume fraction of fibres V_f has some effect on the work of fracture at shorter exposure times but it diminishes as t increases, which is the same trend as for the case of the tensile strength of composites (see Fig. 7). In order to observe the fracture mode of the composites after three-point bending tests, SEM photographs were taken for the composite with V_f = 0.3 and 0.5 and typical fractographs are shown in Fig. 12 for t = 1 h (a) and 72 h (b). It follows from Fig. 12 that the fracture surface at t = 72 h appears flat indicating a brittle fracture pattern while in the fracture surface at t = 1 h a number of fibres which underwent extensive pull-out are quite visible. The above SEM observations are consistent with the values of γ_F measured, i.e. the average values of γ_F at t = 1 and 72 h are 46.4 and 7.2 kJ m^{-2}, respectively.

Next an attempt was made to compare the experimental and analytical results. Though the analytical results were obtained from Equation 15, we have employed two methods to obtain the value of fibre strength, σ_{fu}, and its Weibull modulus, ω, one by DiCarlo's model [7] (Equation 4) and the other by the present experiment. In DiCarlo's model ω was set equal to 5, while the present experimental results on σ_{fu} yielded larger value of ω (see Fig. 9). For both analytical results, a_f was computed by [30]

$$a_f = \left(\frac{wh}{\theta}\right)^{\frac{1}{2}} \tag{20}$$

where w and h denote the width and thickness of the cross-section of the specimen, and θ is the angle (in radians) of the apex of the triangular ligament (see

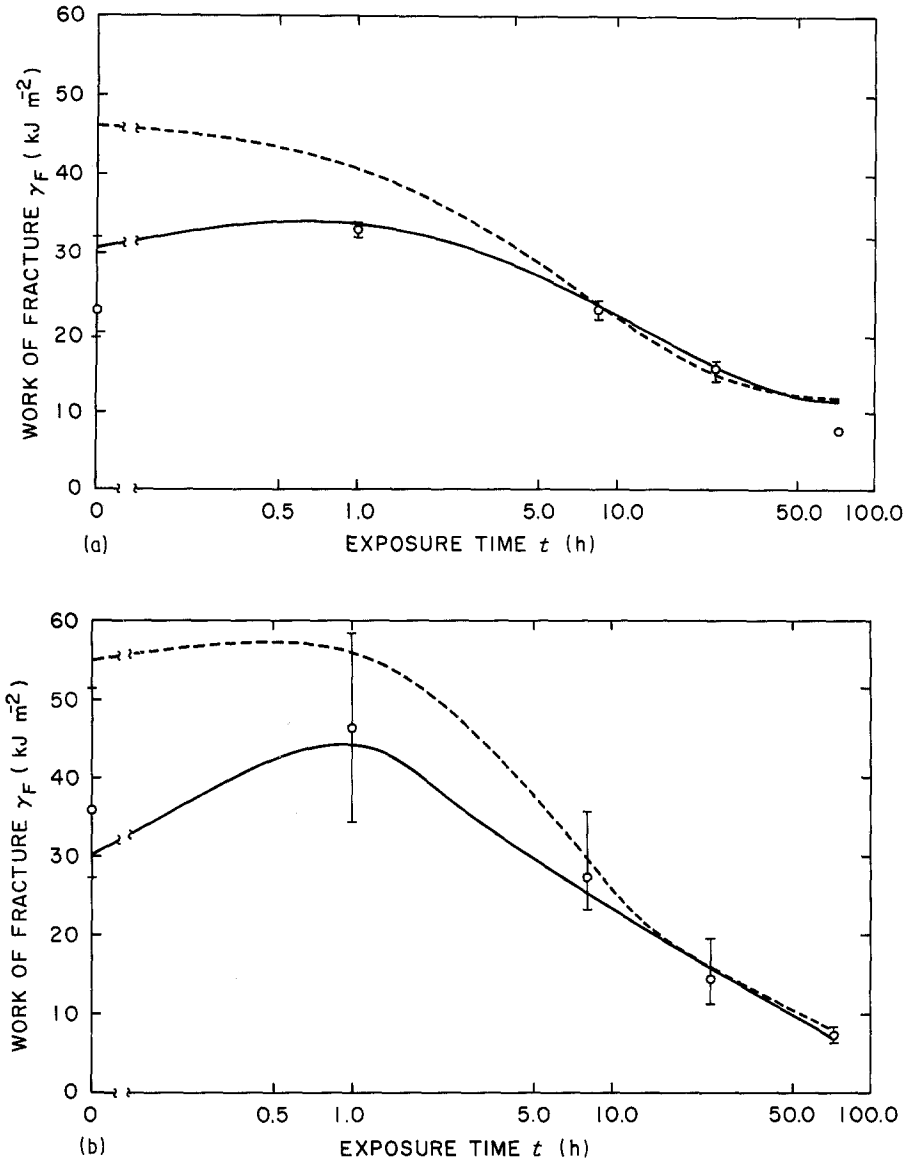

Figure 11 Work of fracture, γ_F, as a function of exposure time, t, for (a) $V_f = 0.3$ and (b) $V_f = 0.5$. (O) Measured by three-point bending test, (———) predicted based on the experimentally obtained ω and σ_{fu}, (– – –) predicted based on DiCarlo's model ($\omega = 5$).

Fig. 1). The analytical results based on the experimentally measured σ_{fu} and DiCarlo's model are plotted as solid and dashed curves, respectively in Fig. 11 for $V_f = 0.3$ (a) and 0.5 (b). In the same figures the experimental results are plotted as open circles with error band. It is clear from Fig. 11 that the analytical results based on DiCarlo's model tend to overestimate γ_F at shorter exposure times t, but they agree well with the experimental ones for larger t, whereas the analytical results based on the experimentally measured σ_{fu} and ω agree well with the experimental ones for the entire range of t.

In order to see the effect of each mechanism among the three mechanisms described in Section 2.2., we have plotted work of fracture (γ_F), strain energy release rate (G), plastic work along the interface (W_p) and fibre pull-out (W_{p0}) as a function of logarithmic exposure time in Fig. 13 for $V_f = 0.3$ (a) and 0.5 (b). It is seen from Fig. 13 that the contribution of the value of G to γ_F is predominant over the other two

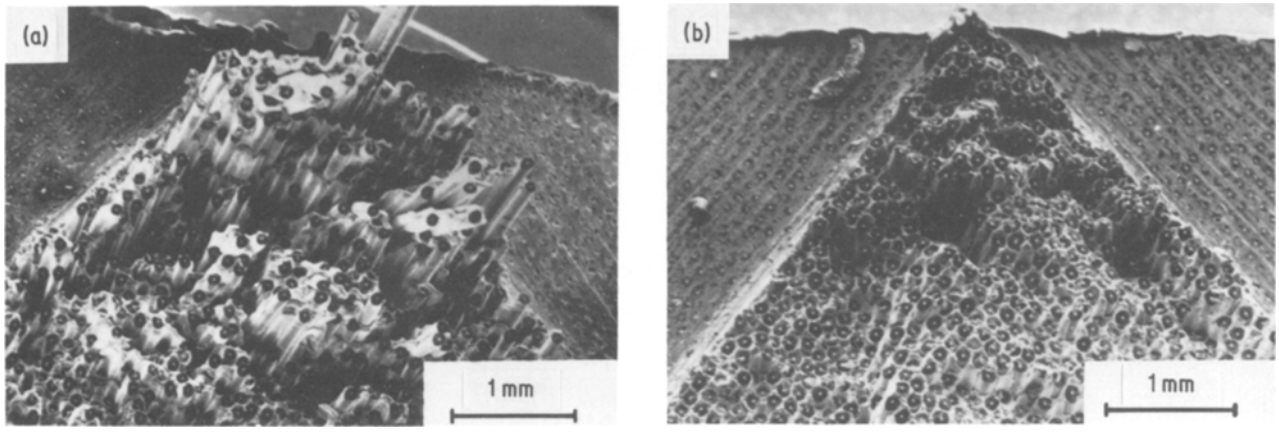

Figure 12 SEM photographs of the fracture surfaces of composite exposed at 500° C, (a) for 1 h and (b) for 72 h.

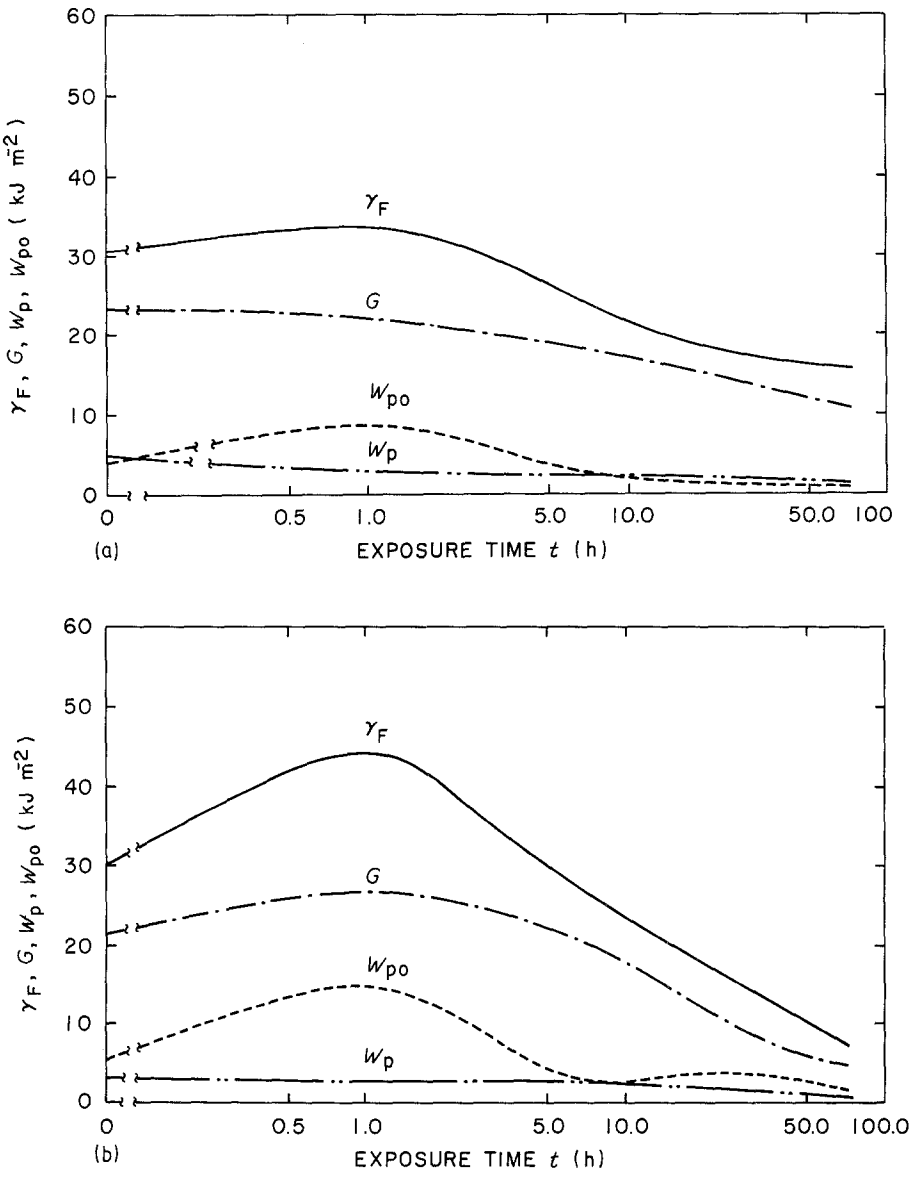

Figure 13 Work of fracture (γ_F), elastic strain energy (G), fibre pull-out energy (W_{p0}) and plastic work (W_p) as a function of exposure time (t) for (a) $V_f = 0.3$ and (b) $V_f = 0.5$

energies and it constitutes 70% of γ_F. It is also noted in these figures that work of fracture is strongly dependent on the distribution of the fibre strength, i.e. the mean value of σ_{fu} and Weibull modulus ω and the ratio of W_{p0}/γ_F tends to increase with V_f.

5. Conclusion

Work of fracture (γ_F) was measured on as-fabricated and as-thermally exposed B/Al composites. Tensile tests were also conducted on the composites and monofilament boron fibres which were extracted from the composite to obtain the strength of composite (σ_c) and fibre (σ_{fu}).

Then the analytical results based on the model of Taya *et al.* were obtained by using two sets of data on the fibre strength σ_{fu} and its Weibull modulus ω, one based on DiCarlo's model ($\omega = 5$) and the other experimentally measured in the present study. Though both predictions agree reasonably well with the experimental results, the prediction based on the experimentally measured σ_{fu} and ω agree very well with the experimental ones for the entire range of exposure time. This implies that DiCarlo's model to predict the fibre strength weakened by isothermal exposure is satisfactory, but it may not be valid for the case of diffusion bonded B/Al where Al_2O_3 film acts as a reaction barrier between boron fibre and aluminium matrix. TEM indicates that there is very little reaction between fibre and matrix in this particular material.

Acknowledgement

We are grateful to Toray Industries, Inc., Japan for its financial support and to the Center for Composite Materials, University of Delaware, for its partial support.

References

1. A. G. METCALFE and M. J. KLEIN, "Interfaces in Metal Matrix Composites, Vol. 1, Composite Materials" edited by A. G. Metcalfe, (Academic Press, New York, 1974) p. 125.
2. M. J. KLEIN and A. G. METCALFE, *AFML* TR-71-189 (1971).
3. *Idem, ibid.* TR-72-226 (1972).
4. M. A. WRIGHT and B. D. INTWALA, *J. Mater. Sci.* **8** (1973) 957.
5. G. C. OLSEN and S. S. TOPKINS, "Failure Modes in Composites IV" edited by J. A. Cornie and F. W. Crossman TMS–AIME, New York, 1979 p. 1.
6. H. H. GRIMES, R. A. LAD and J. E. MAISEL, *Met. Trans. A.* **8A** (1977) 1999.
7. J. A. DICARLO, "Mechanical Behavior of Metal–Matrix Composites" edited by J. E. Hack and M. F. Amateau

(TMS–AIME, New York, 1983) p. 1.
8. M. A. WRIGHT, D. WELCH and J. JOLLAY, *J. Mater. Sci.* **14** (1979) 1218.
9. M. F. KANNIKEN, E. F. RYBICKI and H. F. BRINSON, *Composites* **12** (1977) 17.
10. G. A. COOPER, *Composites* **5** (1970) 645.
11. A. KELLY, *Proc. R. Soc. (Lond.) A.* **319** (1970) 95.
12. D. C. PHILLIPS and A. S. TETELMAN, *Composites* 7 (1972) 216.
13. M. R. PIGGOTT, *J. Mater. Sci.* **5** (1970) 669.
14. J. C. WELLS and P. W. R. BEAUMONT, *ibid.* **17** (1982) 397.
15. E. R. THOMSON, *J. Comp. Mater.* **5** (1971) 235.
16. A. SKINNER, M. J. KOCZAK and A. LAWLEY, *Metall. Trans. A.* **13A** (1982) 289.
17. L. E. DARDI and K. G. KREIDER, "Failure Modes in Composites I" edited by I. Toth (TMS-AIME, New York, 1973) p. 231.
18. M. TAYA and A. DAIMARU, *J. Mater. Sci.* **18** (1983) 3105.
19. A. DAIMARU, T. HATA and M. TAYA, ASTM STP 864 (American Society for Testing and Materials, Philadelphia, 1985) p. 505.
20. J. NAKAYAMA, *Amer. Ceram. Soc. J.* **48** (1965) 583.
21. H. G. TATTERSALL and G. TAPPIN, *J. Mater. Sci.* **1** (1966) 296.
22. H. ISHIKAWA and M. TAYA, Proceedings of ICCM/IV, Vol. 1, edited by T. Hayashi, K. Kawata and S. Umekawa, Japan Society of Composite Materials, Tokyo, 1982, p. 675.
23. H. TADA, P. PARIS and G. IRWIN, "The Stress Analysis of Cracks Handbook" (Del Research Corporation, 1973).
24. B. D. COLEMAN, *J. Mech. Phys. Sol.* **7** (1958) 60.
25. J. M. LIN, P. E. CHEN and A. T. DIBENEDETTO, *Polym. Eng. Sci.* **11** (1971) 344.
26. N. N. GREENWOOD, R. V. PARISH and P. H. THORNTON, *Quart. Rev.* (London.) (1966) 441.
27. W. H. KIM, M. J. KOCZAK and A. LAWLEY, Proceedings of ICCM/2 edited by B. Norton, R. A. Signorelli and K. Street (TMS-AIME, New York, 1978) p. 487.
28. J. A. DICARLO and R. J. SMITH, *NASA* TM-82806 (1982).
29. J. UNNAM, R. N. SHENOY, K. E. WIEDEMANN and R. K. CLARK, 30th National SAMPE Symposium, Advancing Technology in Materials and Processes, Covina, California, 1985, p. 1005.
30. A. DAIMARU, "Stiffness, Strength and Toughness of Metal Matrix Composites: Analytical and Experimental Research", MS thesis, University of Delaware, June 1984.

Received 29 May
and accepted 4 July 1985